


Interaction Effects on the Dynamical Anderson Metal-Insulator Transition Using Kicked Quantum Gases

Jun Hui See Toh¹, Mengxin Du², Xinxin Tang,¹ Ying Su,² Tristan Rojo,¹ Carson O. Patterson,¹ Nicolas R. Williams,¹ Chuanwei Zhang,^{2,3,*} and Subhadeep Gupta^{1,†}

¹*Department of Physics, University of Washington, Seattle, Washington, USA*

²*Department of Physics, The University of Texas at Dallas, Richardson, Texas, USA*

³*Department of Physics, Washington University, St. Louis, Missouri, USA*

 (Received 23 June 2023; revised 12 June 2024; accepted 12 July 2024; published 15 August 2024)

Understanding the interplay of interaction and disorder in quantum transport poses long-standing scientific challenges for theory and experiment. While highly controlled ultracold atomic platforms combining atomic interactions with spatially disordered lattices have led to remarkable advances, the extension of such controlled studies to phenomena in high-dimensional disordered systems, such as the three-dimensional Anderson metal-insulator transition has been limited. Kicked quantum gases provide an alternate experimental platform that captures the Anderson model in momentum space and features dynamical localization as the analog of Anderson localization. Here, we utilize a momentum space lattice platform using quasiperiodically kicked ultracold atomic gases to experimentally investigate interaction effects on the three-dimensional dynamical Anderson metal-insulator transition. We observe interaction-driven subdiffusion and a divergence of delocalization onset time on approaching the phase boundary. Mean-field numerical simulations show qualitative agreement with experimental observations, but with significant quantitative deviations.

DOI: [10.1103/PhysRevLett.133.076301](https://doi.org/10.1103/PhysRevLett.133.076301)

Conceived more than 60 years ago, the celebrated Anderson picture of electron transport in the presence of disorder [1,2] predicts localization in one and two dimensions ($d = 1, 2$), and delocalization in $d > 2$ below a critical minimum disorder, demarcating a metal-insulator transition (MIT). How interparticle interactions compete with disorder during quantum transport has since been the subject of intense theoretical scrutiny [3–6] with to-date unresolved questions surrounding the fate of localized states in the presence of interactions. Interaction effects on localization are challenging to observe in solid-state experiments. Observations in doped semiconductors have been attributed to interaction-driven variable-range hopping, but the mechanism is not fully clear [7,8]. Landmark experiments within the last 15 years with ultracold atoms in spatially disordered optical lattices have observed interaction-driven transport phenomena, such as subdiffusive delocalization [9,10], many-body localization [11–14], and a finite temperature Bose glass-superfluid transition [15]. However, the effects of interactions on quantum transport phenomena in high-dimensional disordered systems, such as the $d = 3$ Anderson MIT [16–18], have largely remained unexplored experimentally in ultracold atomic systems.

In recent years, lattices in the synthetic dimension of momentum space have become a fertile alternate avenue for

dynamical studies and quantum simulation with ultracold atoms [19]. The $d = 1$ Anderson Hamiltonian can be simulated in momentum space using the quantum kicked rotor, where ultracold atoms are periodically driven or “kicked” by a pulsed standing wave and can exhibit the corresponding “dynamical” localization [20–27]. Very recently, experiments have observed the interaction-driven breakdown of this dynamical localization [28,29], shedding light on an area where theoretical results are in contradiction [30,31], further motivating higher-dimensional experiments. By modulating the strength of the kicks, d -dimensional Anderson models can be engineered in the quasiperiodic kicked rotor (QPKR), with the pseudorandom phase accumulated by atoms at different momenta corresponding to the disorder, kick strength to intersite tunneling, and number of modulation frequencies to $d - 1$ [32–35]. The QPKR technique has been utilized experimentally to simulate disordered noninteracting systems in $d = 2$ [36] and $d = 3$, where the Anderson metal-insulator transition was also observed [16]. Recent theoretical works incorporating mean-field interactions predict subdiffusive delocalization in the insulator region of the $d = 3$ model but disagree on the value of the corresponding subdiffusive exponent [37–39].

In this Letter we use the QPKR in conjunction with atomic interaction tuning to experimentally observe interaction-driven delocalization in the insulating region and the interaction-induced shift on the dynamical Anderson MIT in $d = 3$. The transition boundary is manifest as a

*Contact author: chuanwei.zhang@utdallas.edu

†Contact author: deepg@uw.edu

divergence of delocalization onset time with varying kick strength. We study the inverse relation of onset time with interaction strength and also demonstrate interaction-driven delocalization in $d = 2$ and $d = 4$ synthetic space. Our numerical mean-field simulations incorporating system inhomogeneity capture the general trends of our observations, but with quantitative deviations that grow with increasing interaction strength.

Our experimental approach [40] for quantum simulation of the interaction effects on the dynamical Anderson model utilizes Bose-Einstein condensates in the quasi-1D regime that are kicked along the axial (z) direction using a pulsed optical standing wave lattice with period T and pulse width $t_p \ll T$ [see Fig. 1(a)]. $1/T$ is incommensurate with the recoil frequency $\omega_{\text{rec}} = \hbar k_L^2/2m = E_{\text{rec}}/\hbar$, where $k_L = 2\pi/\lambda$ is the wave vector and m is the atom mass. We engineer the d -dimensional Anderson model (for $d = 1$ to 4) in momentum space by modulating the amplitude of these kick pulses with $d - 1$ additional incommensurate frequencies.

A description of the dynamics of the $d = 3$ system with nonlinear mean-field interactions is captured by the

following dimensionless non-linear Gross-Pitaevskii equation (GPE):

$$i\hbar\partial_t\Phi(\theta, \tau) = \left(-\frac{\hbar^2}{2m}\partial_\theta^2 + \frac{1}{2}\omega_\theta^2\theta^2 + g|\Phi(\theta, \tau)|^2 - K(1 + \varepsilon \cos \omega_2\tau \cos \omega_3\tau) \times \cos \theta \sum_{n_p} \delta(\tau - n_p) \right) \Phi(\theta, \tau), \quad (1)$$

where Φ is the wave function, $\hbar = 8\omega_{\text{rec}}T$ is the reduced Planck constant, $\theta = 2k_L z$ and $\tau = t/T$ are the position and time parameters, and n_p is the pulse number. The axial frequency is $\omega_\theta = \omega_z T$ and the initial peak density is $n_{1D} = |\Phi(0, 0)|^2 = \bar{n}_{1D}/2k_L$, where the wave function is normalized as $\int d\theta |\Phi(\theta, \tau)|^2 = N_{\text{atom}}$. The kick strength K and interaction constant g are defined as

$$K = 4s_z\omega_{\text{rec}}^2 t_p T, \quad g = \frac{2\bar{g}k_L\hbar T}{\hbar} = \hbar^2 \frac{k_L a_s}{(k_L a_\perp)^2}, \quad (2)$$

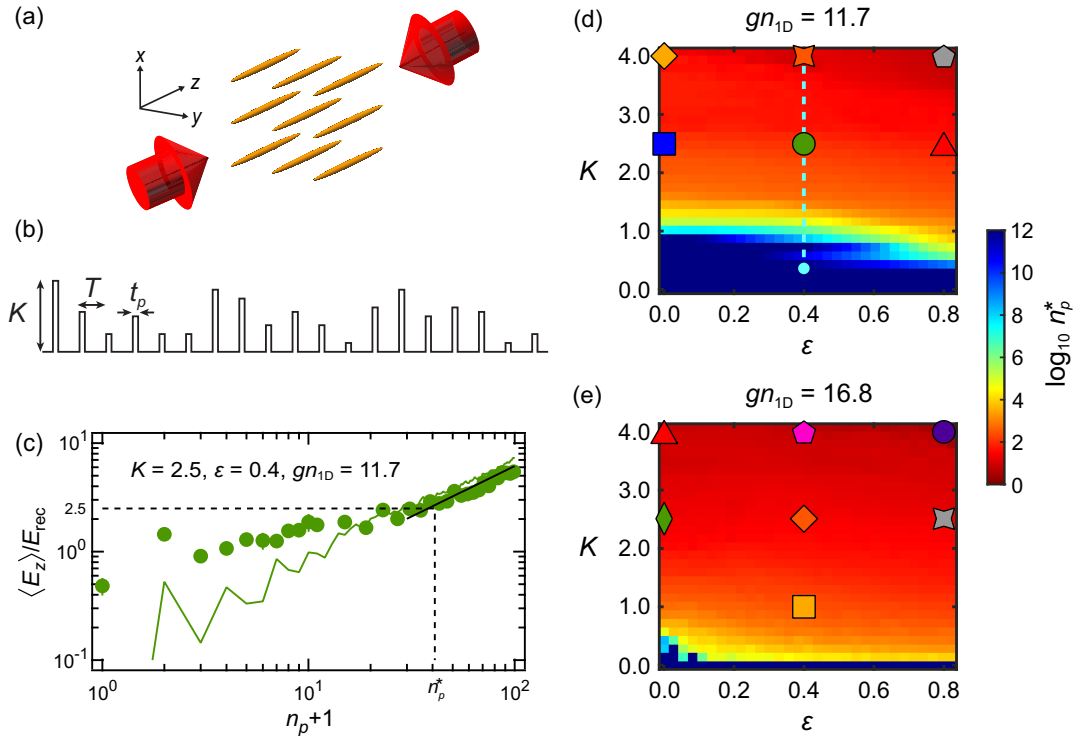


FIG. 1. Experimental scheme and phase diagrams for the $d = 3$ dynamical Anderson model with different nonlinear interaction strengths. (a) Experimental schematic showing BECs in 1D tubes with kicking pulses applied along the axial (z) direction. (b) Schematic of quasiperiodic drive of optical standing wave pulses to engineer the $d = 3$ Anderson model. (c) Evolution of axial kinetic energy corresponding to $K = 2.5$, $\varepsilon = 0.4$, and $gn_{1D} = 11.7$. The dashed lines mark $E^* = 2.5E_{\text{rec}}$ and the corresponding n_p^* . Also shown is the GPE simulation (colored line) and a power law fit with an exponent of 0.70(2) (black solid line). In (d) and (e) we show the numerically simulated phase diagrams of the interacting $d = 3$ dynamical Anderson model using the Gross-Pitaevskii equation for two different interaction strengths $gn_{1D} = 11.7$ and 16.8. The sharp change in the delocalization onset time n_p^* marks the dynamical Anderson MIT. Markers indicate where $d = 3$ delocalization data was collected (Figs. 2–4) and the dashed line indicates the line along which the interacting dynamical Anderson transition was observed (Fig. 2).

where $s_z E_{\text{rec}}$ is the peak depth of the pulsed optical lattice. K is modulated by incommensurate frequencies ω_2 and ω_3 (in units of $1/T$) with modulation strength ε .

In the absence of interactions and axial confinement, and for $\varepsilon = 0$, the Hamiltonian of Eq. (1) is the periodic kicked rotor that maps to the $d = 1$ Anderson Hamiltonian in momentum space, and exhibits the corresponding dynamical localization [34]. The K parameter controls the tunneling between sites in the momentum lattice and a pseudorandom phase at each site arises from the period T being incommensurate with $1/\omega_{\text{rec}}$. For $\varepsilon \neq 0$ and incommensurate ω_2, ω_3 , the mapping is to a $d = 3$ Anderson model in momentum space, detailed in Sec. IV of the Supplemental Material [40]. The ε parameter modulates K and controls intersite tunneling along the two additional synthetic dimensions. Thus, n_p is the time variable, K is related to the hopping in all dimensions, and ε is related to the hopping in all but one dimension in this mapping to the Anderson model. The interaction term in Eq. (1) becomes infinitely long-ranged in the momentum-space lattice [28]. This nonlocal interaction in the synthetic momentum space is significantly different from the local interacting disorder problems discussed in the condensed matter context [7,8].

Throughout this Letter, we use $\omega_2 = 2\pi \times \sqrt{2}$ and $\omega_3 = 2\pi \times \sqrt{3}$ [see Fig. 1(b)], with $t_p = 4 \mu\text{s}$, $T = 105 \mu\text{s}$ and $k = 5.26$, for our QPKR realization of the $d = 3$ Anderson model. The interaction strength gn_{1D} is controlled experimentally through a_{\perp} , the transverse oscillator length of confinement [40].

In a typical experimental sequence, after the desired pulse number n_p , we diabatically turn off the trapping potential and take a time-of-flight absorption image along x [40]. The axial momentum distribution is obtained by integrating the distribution along y . The axial kinetic energy of the atoms $\langle E_z \rangle$ is then calculated from this momentum distribution. Figure 1(c) shows an example of evolution of $\langle E_z \rangle$ with n_p . Fitting a power law to the long time evolution $\langle E_z \rangle = E_0(n_p)^\alpha$ allows extraction of α and E_0 .

In Figs. 1(d) and 1(e), we show the numerically simulated $K - \varepsilon$ phase diagram for two different interaction strengths, where the transition from a localized insulating phase to a delocalized metallic phase can be clearly identified across a sharp phase boundary [40]. To remove unimportant single-particle features arising from the harmonic oscillator timescale and the finite depth trap [40,43], and more clearly reveal the effects of interactions, we display the phase diagrams through the delocalization onset time n_p^* rather than the diffusive exponent. Importantly, the interaction-shifted dynamical Anderson MIT boundaries are in agreement for either parameter choice [40].

We define the onset time n_p^* as the pulse number at which the average energy $\langle E_z \rangle$ of a system undergoing delocalization reaches E^* , chosen to be much larger than the initial

energy. For an evolution governed by $\langle E_z \rangle = E_0(n_p)^\alpha$ with diffusive exponent α , $n_p^* = (E^*/E_0)^{1/\alpha}$ is directly related to the inverse of the diffusion constant E_0 , whose divergent behavior is used to characterize the MIT phase boundary on the metal side in the homogeneous noninteracting case [33]. In our inhomogeneous system, we use n_p^* for this characterization, with the insulator phase corresponding to $n_p^* \rightarrow \infty$. α and E_0 are the slope and intercept respectively on the log-log plot of $\langle E_z \rangle$ vs n_p , and can also be obtained from the $\langle E_z \rangle$ values at two different n_p [40]. Throughout this Letter we define n_p^* using $E^* = 2.5E_{\text{rec}}$, a sufficiently large value that also provides an adequate dynamic range for data analysis [see Fig. 1(c)]. The insulating regions of the phase diagrams in Figs. 1(d) and 1(e) are far smaller than that of the noninteracting homogeneous dynamical Anderson model [16,44], with the higher interaction strength showing a smaller insulating region.

We present our observation of an interacting dynamical Anderson MIT in Fig. 2 where sequences of absorption images for $n_p = 0, 30, 100$ [Figs. 2(a)–2(c)] show the growth in the axial (z) momentum distribution [$n_p = 100$ cases shown in Fig. 2(d)] for different kick strengths K , with fixed interaction strength $gn_{1D} = 11.7$ and $\varepsilon = 0.4$. A clear progression from insulating (localized) to metal (delocalized) behavior emerges as the K parameter is increased. From the corresponding $\langle E_z \rangle$ [Fig. 2(d)], the dependence of n_p^* on K can be determined. We observe a divergence of n_p^* as K is varied with $gn_{1D} = 11.7$ and $\varepsilon = 0.4$ [Fig. 2(e)], which marks the phase transition boundary. Our numerical mean-field simulations (green line) capture the general trend of the experimental observations.

In Fig. 3, we show the evolution of the axial kinetic energy of the system for a few different combinations of ε , K , and gn_{1D} , corresponding to various locations in the phase diagrams of Fig. 1. In all of these cases, localization is predicted in the noninteracting homogeneous case [16,44], while we observe delocalization. This emphasizes the role of interactions on the MIT phase diagram. We find qualitative agreement with our GPE simulations (colored solid lines). Simulation results setting $g = 0$ (colored dashed lines) show order-of-magnitude lower energies at long times with small temporal variation stemming from the inhomogeneous weak axial harmonic confinement.

Power law fits return exponents $\alpha \in \{0.6, 1.1\}$, and are predominantly subdiffusive. These values characterize all our observations shown in the main text and also additional data included in the Supplemental Material [40], and are larger than mean-field theory predictions for a homogeneous system [37,38]. We note that small regions with $\alpha > 1$ also exist in the parameter space explored in our inhomogeneous system [40].

To more systematically analyze the interaction dependence, we fix kick and modulation strengths to representative values $K = 2.5$ and $\varepsilon = 0.4$, and study the evolution of

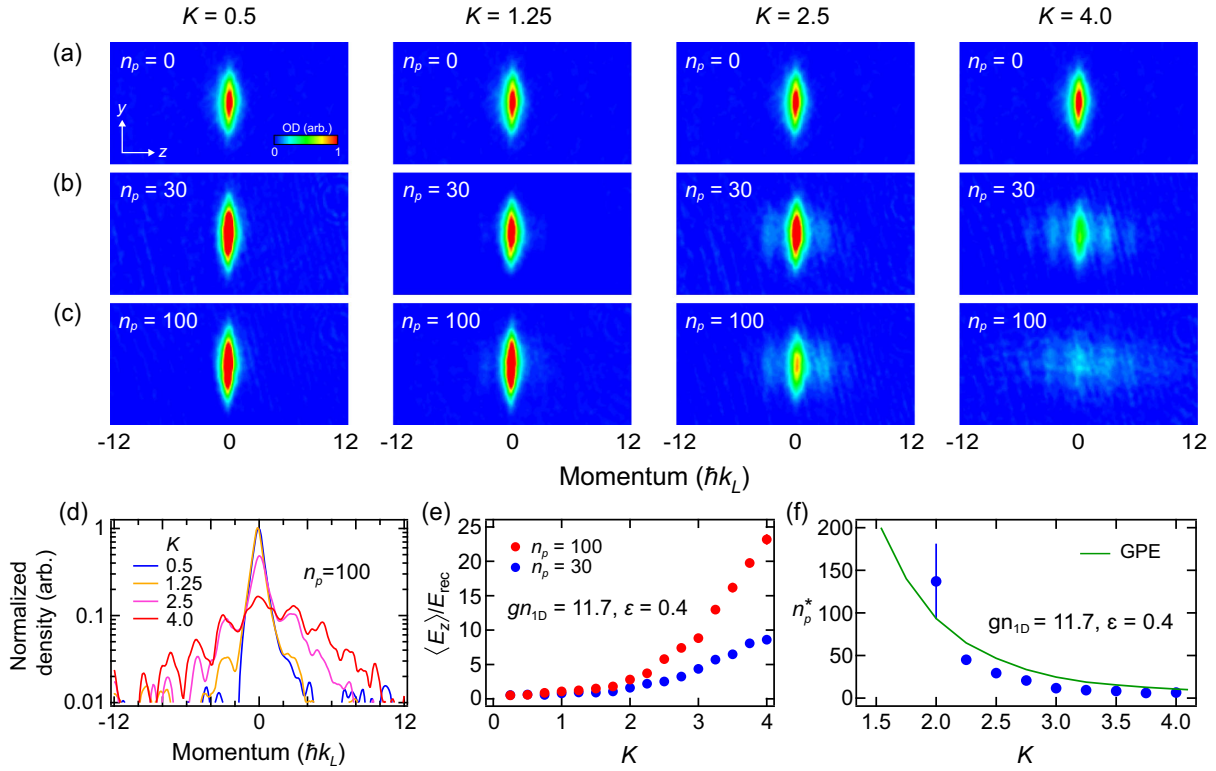


FIG. 2. Observing the interacting dynamical Anderson MIT in three-dimensional synthetic momentum space. (a)–(c) Sequence of absorption images for $n_p = 0, 30, 100$ showing the transition from localized to delocalized evolution as K is varied from 0.5–4.0 for $gn_{1D} = 11.7$ and $\epsilon = 0.4$. The time of flight for all images is 15 ms. The kicks are applied along the horizontal (z) direction coinciding with the axis of the 1D gas. (d) Axial momentum distribution corresponding to the $n_p = 100$ absorption images shown in panel (c). (e) Calculated $\langle E_z \rangle$ for $n_p = 30$ and 100, with $gn_{1D} = 11.7$, $\epsilon = 0.4$, at various kick strengths K . (f) Divergence of n_p^* as K approaches a critical value. The green line shows the mean-field theory result.

axial energy with kick number across a range of interaction strengths. The time evolution of both $gn_{1D} = 11.7$ and 16.8 cases in Fig. 4(a) exhibit delocalization with a small difference in character.

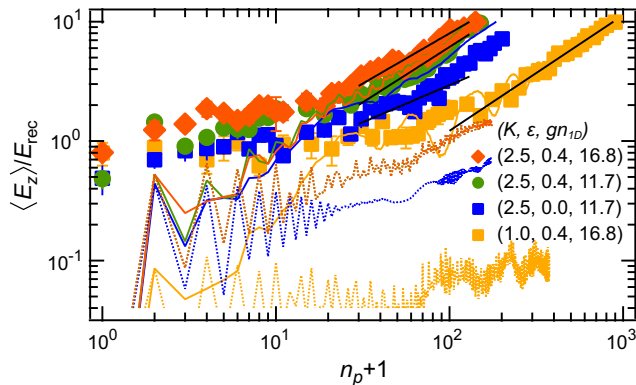


FIG. 3. Evolution of axial kinetic energy $\langle E_z \rangle$ with pulse number n_p for different modulation strengths ϵ and kick strengths K . The colored solid lines are the corresponding numerical simulations using the GPE. The colored dashed lines are the corresponding noninteracting numerical simulations setting $g = 0$. The black solid lines are power law fits to the data.

The interaction dependence can be more sensitively detected using onset time n_p^* as the metric, rather than long-time energy diffusion. In Fig. 4(b) we show how n_p^* changes as we vary the interaction strength by tuning the external confinement and thus a_{\perp} . We observe a monotonically decreasing delocalization onset time with stronger interaction strength. The deviation from our mean-field numerical model [green line in Fig. 4(b)] is significant and increases with interaction strength. We note that since we do not start experimentally in the true ground state (85% initial condensate fraction [40]) unlike in the simulation, the absolute value of n_p^* is not directly comparable between experiment and mean-field theory, and the deviations in Fig. 4(b) provide only qualitative trends with interactions.

By experimentally realizing an interacting QPKR Hamiltonian simulator, we investigated interaction effects on the dynamical Anderson metal-insulator transition. A $d = 3$ interacting Anderson MIT was observed as a divergence in the delocalization onset time, a measure of the inverse diffusion rate. Measured subdiffusive delocalization exponents in the metal phase exceed prior mean-field theory predictions for the homogeneous case. Incorporating experimental inhomogeneity into the mean-field theory, we find qualitative agreement with our observations with deviations

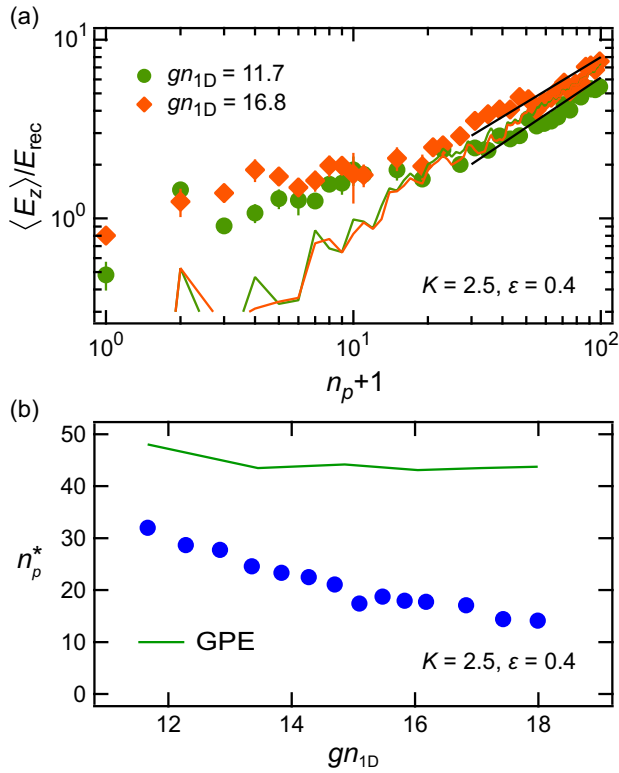


FIG. 4. Tuning interaction strength in the $d = 3$ dynamical Anderson model. (a) Evolution of axial kinetic energy $\langle E_z \rangle$ with pulse number n_p for different interaction strengths gn_{1D} . The colored solid lines are the corresponding numerical simulations using the GPE. The black solid lines are power law fits to the data. (b) Onset of delocalization n_p^* as a function of interaction strength gn_{1D} . The green solid line shows the numerical simulation using the GPE.

increasing with interaction strength. Using the flexibility of the momentum-space approach, we have also engineered Anderson models in other dimensions ($d = 1-4$) and observed interaction-driven subdiffusive delocalization of the insulator phase with shorter onset time at larger interaction strength [40]. Our combined experiment-theory collaboration advances the area of many-body quantum simulation of high-dimensional quantum transport, while revealing the need for a beyond mean-field theoretical description to address the infinitely long-range interaction in momentum space [28]. While the long-range nature of the interaction is different from the conventional discussion of the Anderson model in solid-state physics, Coulomb interactions in disordered lattices have been investigated in recent work [45]. Furthermore, this feature of our work also makes it relevant in the context of dipolar [46] or trapped-ion [47] quantum systems where the long-range interactions can be examined and harnessed for applications in quantum information science [48].

Future work includes experimental realization of the interacting QPKR in a homogeneous 1D system, such as a ring trap [49–52] or box trap [53], where potential

universality [37] of the subdiffusive exponent α can be tested, critical exponents for the interacting phase transition can be accurately measured, and the fate of the interacting dynamical Anderson MIT can be examined in a homogeneous setting. Further studies of the nature of many-body transport phases can be pursued with a larger interaction tuning range using a magnetic Feshbach resonance [29,54]. The technique of kicked quantum gases is well suited for studying the interplay of disorder, interactions and dimensionality in quantum transport, and fruitful applications to other ultracold many-body systems such as the Tonks gas [55] and strongly interacting fermions [56] are envisioned.

Acknowledgments—We thank M. Rudner, C. R. Laumann, and A. Chandran for helpful discussions. Work at the University of Washington is supported by the Air Force Office of Scientific Research (FA9550-22-1-0240). N. R. W. acknowledges support from an NDSEG fellowship. C. O. P. acknowledges support from NSF-NRT Grant No. DGE-2021540. T. R. acknowledges support from the NSF-REU program at the University of Washington (Grant No. NSF-REU 1851741). Work at the University of Texas at Dallas is supported by the Air Force Office of Scientific Research (FA9550-20-1-0220), Army Research Office (No. W911NF-17-1-0128), Department of Energy (DESC0022069), and National Science Foundation (No. PHY-2409943, No. OMR-2228725).

- [1] P. W. Anderson, Absence of diffusion in certain random lattices, *Phys. Rev.* **109**, 1492 (1958).
- [2] E. Abrahams, P. W. Anderson, D. C. Licciardello, and T. V. Ramakrishnan, Scaling theory of localization: Absence of quantum diffusion in two dimensions, *Phys. Rev. Lett.* **42**, 673 (1979).
- [3] L. Fleishman and P. W. Anderson, Interactions and the Anderson transition, *Phys. Rev. B* **21**, 2366 (1980).
- [4] T. Nattermann, T. Thierry Giamarchi, and P. Le Doussal, Variable-range hopping and quantum creep in one dimension, *Phys. Rev. Lett.* **91**, 056603 (2003).
- [5] I. V. Gornyi, A. D. Mirlin, and D. G. Polyakov, Dephasing and weak localization in disordered Luttinger liquid, *Phys. Rev. Lett.* **95**, 046404 (2003).
- [6] D. Basko, I. Aleiner, and B. Altshuler, Metal-insulator transition in a weakly interacting many-electron system with localized single-particle states, *Ann. Phys. (Amsterdam)* **321**, 1126 (2006).
- [7] A. Lagendijk, B. van Tiggelen, and D. Wiersma, Fifty years of Anderson localization, *Phys. Today* **62**, No. 8, 24 (2009).
- [8] *50 Years of Anderson Localization*, edited by Elihu Abrahams (World Scientific, Singapore, 2010).
- [9] B. Deissler, M. Zaccanti, G. Roati, C. D’Errico, M. Fattori, M. Modugno, G. Modugno, and M. Inguscio, Delocalization of a disordered bosonic system by repulsive interactions, *Nat. Phys.* **6**, 354 (2010).
- [10] E. Lucioni, B. Deissler, L. Tanzi, G. Roati, M. Zaccanti, M. Modugno, M. Larcher, F. Dalfovo, M. Inguscio, and

- G. Modugno, Observation of subdiffusion in a disordered interacting system, *Phys. Rev. Lett.* **106**, 230403 (2011).
- [11] M. Schreiber, S. S. Hodgman, P. Bordia, H. P. Lüschen, M. H. Fischer, R. Vosk, E. Altman, U. Schneider, and I. Bloch, Observation of many-body localization of interacting fermions in a quasirandom optical lattice, *Science* **349**, 842 (2015).
- [12] H. P. Lüschen, P. Bordia, S. Scherg, F. Alet, E. Altman, U. Schneider, and I. Bloch, Observation of slow dynamics near the many-body localization transition in one-dimensional quasiperiodic systems, *Phys. Rev. Lett.* **119**, 260401 (2017).
- [13] A. Lukin, M. Rispoli, R. Schittko, M. E. Tai, A. M. Kaufman, S. Choi, V. Khemani, J. Léonard, and M. Greiner, Probing entanglement in a many-body-localized system, *Science* **364**, 256 (2019).
- [14] S. S. Kondov, W. R. McGehee, W. Xu, and B. DeMarco, Disorder-induced localization in a strongly correlated atomic Hubbard gas, *Phys. Rev. Lett.* **114**, 083002 (2015).
- [15] C. Meldgin, U. Ray, P. Russ, D. Chen, D. Ceperley, and B. DeMarco, Probing the Bose glass-superfluid transition using quantum quenches of disorder, *Nat. Phys.* **12**, 646 (2016).
- [16] J. Chabé, G. Lemarie, B. Gremaud, D. Delande, P. Szriftgiser, and J. C. Garreau, Experimental observation of the Anderson transition with atomic matter waves, *Phys. Rev. Lett.* **101**, 255702 (2008).
- [17] S. Kondov, W. McGehee, J. Zirbel, and B. DeMarco, Three-dimensional Anderson localization of ultracold matter, *Science* **307**, 1296 (2011).
- [18] F. Jendrzejewski, A. Bernard, K. Müller, P. Cheinet, V. Josse, M. Piraud, L. Pezzé, L. Sanchez-Palencia, A. Aspect, and P. Bouyer, Three-dimensional localization of ultracold atoms in an optical disordered potential, *Nat. Phys.* **8**, 398 (2012).
- [19] E. J. Meier, A. A. Fangzhao, A. Dauphin, M. Maffei, P. Massignan, T. L. Hughes, and B. Gadway, Observation of the topological Anderson insulator in disordered atomic wires, *Science* **362**, 929 (2018).
- [20] F. L. Moore, J. C. Robinson, C. Bharucha, P. E. Williams, and M. G. Raizen, Observation of dynamical localization in atomic momentum transfer: A new testing ground for quantum chaos, *Phys. Rev. Lett.* **73**, 2974 (1994).
- [21] F. L. Moore, J. C. Robinson, C. F. Bharucha, B. Sundaram, and M. G. Raizen, Atom optics realization of the quantum δ -kicked rotor, *Phys. Rev. Lett.* **75**, 4598 (1995).
- [22] M. B. d'Arcy, R. M. Godun, M. K. Oberthaler, D. Cassettari, and G. S. Summy, Quantum enhancement of momentum diffusion in the delta-kicked rotor, *Phys. Rev. Lett.* **87**, 074102 (2001).
- [23] H. Ammann, R. Gray, I. Shvarchuck, and N. Christensen, Quantum delta-kicked rotor: Experimental observation of decoherence, *Phys. Rev. Lett.* **80**, 4111 (1998).
- [24] S. Wimberger, I. Guarneri, and S. Fishman, Quantum resonances and decoherence for delta-kicked atoms, *Nonlinearity* **16**, 1381 (2003).
- [25] G. J. Duffy, A. S. Mellish, K. J. Challis, and A. C. Wilson, Nonlinear atom-optical δ -kicked harmonic oscillator using a Bose-Einstein condensate, *Phys. Rev. A* **70**, 041602(R) (2004).
- [26] A. Ullah, S. Reddel, J. Currivan, and M. D. Hoogerland, Quantum resonant effects in the delta-kicked rotor revisited, *Eur. Phys. J. D* **66** (2012).
- [27] B. Gadway, J. Reeves, L. Krinner, and D. Schneble, Evidence for a quantum-to-classical transition in a pair of coupled quantum rotors, *Phys. Rev. Lett.* **110**, 190401 (2013).
- [28] J. See Toh, K. C. McCormick, X. Tang, Y. Su, X. Luo, C. Zhang, and S. Gupta, Many-body dynamical delocalization in a kicked one-dimensional ultracold gas, *Nat. Phys.* **18**, 1297 (2022).
- [29] A. Cao, R. Sajjad, H. Mas, E. Q. Simmons, J. L. Tanlimco, E. Nolasco-Martinez, T. Shimasaki, H. E. Kondakci, V. Galitski, and D. M. Weld, Interaction-driven breakdown of dynamical localization in a kicked quantum gas, *Nat. Phys.* **18**, 1302 (2022).
- [30] S. Lellouch, A. Rançon, S. De Bièvre, D. Delande, and J. C. Garreau, Dynamics of the mean-field-interacting quantum kicked rotor, *Phys. Rev. A* **101**, 043624 (2020).
- [31] C. Rylands, E. B. Rozenbaum, V. Galitski, and R. Konik, Many-body dynamical localization in a kicked Lieb-Liniger gas, *Phys. Rev. Lett.* **124**, 155302 (2020).
- [32] G. Casati, I. Guarneri, and D. L. Shepelyansky, Anderson transition in a one-dimensional system with three incommensurate frequencies, *Phys. Rev. Lett.* **62**, 345 (1989).
- [33] G. Lemarié, J. Chabé, P. Szriftgiser, J. C. Garreau, B. Grémaud, and D. Delande, Observation of the Anderson metal-insulator transition with atomic matter waves: Theory and experiment, *Phys. Rev. A* **80**, 043626 (2009).
- [34] S. Fishman, D. R. Grempel, and R. E. Prange, Chaos, quantum recurrences, and Anderson localization, *Phys. Rev. Lett.* **49**, 509 (1982).
- [35] D. R. Grempel, R. E. Prange, and S. Fishman, Quantum dynamics of a nonintegrable system, *Phys. Rev. A* **29**, 1639 (1984).
- [36] I. Manai, J.-F. Clément, R. Chicireanu, C. Hainaut, J. C. Garreau, P. Szriftgiser, and D. Delande, Experimental observation of two-dimensional Anderson localization with the atomic kicked rotor, *Phys. Rev. Lett.* **115**, 240603 (2015).
- [37] N. Cherroret, B. Vermersch, J. C. Garreau, and D. Delande, How nonlinear interactions challenge the three-dimensional Anderson transition, *Phys. Rev. Lett.* **112**, 170603 (2014).
- [38] L. Ermann and D. Shepelyansky, Destruction of Anderson localization by nonlinearity in kicked rotator at different effective dimensions, *J. Phys. A* **47**, 335101 (2014).
- [39] B. Vermersch, D. Delande, and J. C. Garreau, Bogoliubov excitations in the quasiperiodic kicked rotor: Stability of a kicked condensate and the quasi-insulator-to-metal transition, *Phys. Rev. A* **101**, 053625 (2020).
- [40] See Supplemental Materials at <http://link.aps.org/supplemental/10.1103/PhysRevLett.133.076301> for more experimental and theoretical details, which includes Refs. [41–42].
- [41] R. Roy, A. Green, R. Bowler, and S. Gupta, Rapid cooling to quantum degeneracy in dynamically shaped atom traps, *Phys. Rev. A* **93**, 043403 (2016).
- [42] R. Roy, A. Green, R. Bowler, and S. Gupta, Two-element mixture of Bose and Fermi superfluids, *Phys. Rev. Lett.* **118**, 055301 (2017).

- [43] T. P. Billam and S. A. Gardiner, Quantum resonances in an atom-optical δ -kicked harmonic oscillator, *Phys. Rev. A* **80**, 023414 (2009).
- [44] M. Lopez, J. Clement, G. Lemarie, D. Delande, P. Szriftgiser, and J. C. Garreau, Phase diagram of the anisotropic Anderson transition with the atomic kicked rotor: Theory and experiment, *New J. Phys.* **15**, 065013 (2013).
- [45] A. Marie, D. P. Kooi, J. Grossi, M. Seidl, Z. H. Musslimani, K. J. H. Giesbertz, and P. Gori-Giorgi, Real-space Mott-Anderson electron localization with long-range interactions, *Phys. Rev. Res.* **4**, 043192 (2022).
- [46] C. Holland, Y. Lu, and L. Cheuk, On-demand entanglement of molecules in a reconfigurable optical tweezer array, *Science* **382**, 1143 (2023).
- [47] C. Bruzewicz, J. Chiaverini, R. McConnell, and J. Sage, Trapped-ion quantum computing: Progress and challenges, *Appl. Phys. Rev.* **6**, 021314 (2019).
- [48] Z. X. Gong, M. Foss-Feig, S. Michalakis, and A. V. Gorshkov, Persistence of locality in systems with power-law interactions, *Phys. Rev. Lett.* **113**, 030602 (2014).
- [49] A. Ramanathan, K. C. Wright, S. R. Muniz, M. Zelan, W. T. Hill, C. J. Lobb, K. Helmerson, W. D. Phillips, and G. K. Campbell, Superflow in a toroidal Bose-Einstein condensate: An atom circuit with a tunable weak link, *Phys. Rev. Lett.* **106**, 130401 (2011).
- [50] S. Eckel, A. Kumar, T. Jacobson, I. B. Spielman, and G. K. Campbell, Rapidly expanding Bose-Einstein condensate: An expanding universe in the lab, *Phys. Rev. X* **8**, 021021 (2018).
- [51] Y. Cai, D. G. Allman, P. Sabharwal, and K. C. Wright, Persistent currents in rings of ultracold fermionic atoms, *Phys. Rev. Lett.* **128**, 150401 (2022).
- [52] G. Del Pace, K. Khani, A. Muzi Falconi, M. Fedrizzi, N. Grani, D. Hernandez Rajkov, M. Inguscio, F. Scazza, W. J. Kwon, and G. Roati, Imprinting persistent currents in tunable fermionic rings, *Phys. Rev. X* **12**, 041037 (2022).
- [53] A. L. Gaunt, T. F. Schmidutz, I. Gotlibovych, R. P. Smith, and Z. Hadzibabic, Bose-Einstein condensation of atoms in a uniform potential, *Phys. Rev. Lett.* **110**, 200406 (2013).
- [54] C. Chin, R. Grimm, P. S. Julienne, and E. Tiesinga, Feshbach resonances in ultracold gases, *Rev. Mod. Phys.* **82**, 1225 (2010).
- [55] V. Vuatelet and A. Raçon, Effective thermalization of a many-body dynamically localized Bose gas, *Phys. Rev. A* **104**, 043302 (2021).
- [56] M. Messer, K. Sandholzer, F. Görg, J. Minguzzi, R. Desbuquois, and T. Esslinger, Floquet dynamics in driven Fermi-Hubbard systems, *Phys. Rev. Lett.* **121**, 233603 (2018).